Seismic Based Characterization of Baturaja Carbonate at 3D Topaz Area*

Indra Yuliandri[1], Totong Usman[2], and Muharram Panguriseng[2]

Search and Discovery Article #50531 (2012)
Posted January 9, 2012

*Adapted from extended abstract prepared in conjunction with poster presentation at AAPG International Convention and Exhibition, Milan, Italy, October 23-26, 2011

[1]Eksploration, PT. PERTAMINA EP, Jakarta, Indonesia (d_12_a@yahoo.com)
[2]Eksploration, PT. PERTAMINA EP, Jakarta, Indonesia

Abstract

The Early Miocene Baturaja Formation is one of the principal reservoirs in the 3D Topaz area. The original facies distribution of the carbonate reservoir has the tendency for significant horizontal and vertical heterogeneity over short distance, so provide a challenge for seismic interpretation and reservoir characterization. Based on data from several wells, carbonate platform of Baturaja Formation at 3D Topaz area shows different lateral facies change, contain evidence of diagenesis, and fracturation process which affect the reservoir quality. Reservoir characterization made from interpolating well data are too simple to predict reservoir propeties accurately, so the seismic data can help reduce uncertainty about rock properties among wells. Seismic facies and geometries interpreted from the attribute analyses and seismic inversion combined with interpretation of the original seismic, cutting-core log data, and geological interpretation allowed construction of robust structural and depositional models of carbonate environments. The results of the inversion were acoustic impedance and porosity derived from the simple relationship between porosity and acoustic impedance as observed from the well data. The results were used to interpret the facies distribution and to map the porosity distribution. By adding careful hydrocarbon distribution interpretation, the inversion results have been used for locating new wells to drill for hydrocarbons.

Introduction

3D seismic allows us to extrapolate point source information from the wells and hence to investigate the platform geometry and its build-up development. Vertical seismic data resolution in carbonate reservoirs is significantly less than in siliciclastic reservoirs because carbonate rocks have higher velocities and greater densities. Therefore, the seismic data for carbonate at 3D Topaz area with high seismic P-wave velocities (over 4000 m/s) and dominant frequencies 25 Hz have a vertical resolution of approximately 50 m. Thus must be interpreted within the context of a depositional model and integrated with all of the other available data to build a reasonable carbonate reservoir characterisation. Geologically, the study area is located in South Palembang Sub Basin, South Sumatra Basin (Figure 1).

Methodology and Result

Well Correlation

The Baturaja Limestone cycles were recognized and correlated based on lithology and facies. Well log correlation at 3D Topaz area was done based on cyclicity concept and showed two cycles (Figure 1). Cyclicity concept focusses on the significance of sea level change in predicting the lithology and hydrocarbon potential in depositional systems.

The first cycle of Baturaja Limestone was found in all wells at 3D Topaz area while the second cycle was not observed at several wells. From the gamma-ray log, a clear differentiation can be made between the first cycle and second cycle. The gamma-ray responses gradually increase from top of first cycle to second cycle. The sea level relative changes have occurred repeatedly and cyclically through geological time. The rate of relative sea level rises has an obvious effect on the sediment type and the nature of deposition, whereas the rate and extent of relative sea level fall has a marked effect on the diagenesis and erosion of carbonate sequences. The response of the carbonate depositional surface to relative sea level changes include drowning of the surface, catching up with sea level rise, keeping up with the rise, or build up to exposure.The first cycle carbonate stages was started during transgressive of sea level periods of shallow water deposition to fill accommodation place over the platform. Based on information taken from well cutting and core description, the western part of 3D Topaz area was dominated by mudstone/wackstone, center part was dominated by boundstone/wackstone/packstone which indicate reefal area and eastern part was dominated by wackstone/packstone, refer to classification of carbonate from Dunham (1962). This transgressive sea level rise period was still continued until the carbonate reached the top of first cycle. After that, sea level was dropped and the carbonate exsposed to the surface, and followed by diagenetic process. Diagenetic features shows from Figure 2, where the vuggy porosity creation in the upper part of the first cycle have been associated with meteoric diagenesis. RHOB log also shows good porosity development in the upper part of the first cycle. However, in the lower part diagenetic process was not well developed as in the upper part. This is due to the fact that the diagenetic dissolution to create a secondary porosity both in meteoric vadose zone and phreatic zone which were excellently developed in the upper part were relatively negligible in the lower part zone. The second cycle carbonate stages was started when sea level rise again to fill the space. Based on cutting description and gradual increase of gamma-ray log, carbonate in the second cycle was dominated by mudstone. When sea level dropped again, diagenetic process was developed in this cycle. This is showed by the chalky cutting description, indicating the influence of the meteoric pore water input. The vuggy porosity was, however, not well developed. RHOB log also shows that the carbonate rocks within cycle two is a tight limestone. Because of the broad-spectrum of diagenesis that affects carbonate rocks, the final porosity in carbonates may or may not be related to depositional environment. Figure 3 shows the secondary porosity development like vuggy porosity and fracturation in Baturaja Limestone at the study area.

From well correlation, it is clearly seen that the Baturaja Limestone at 3D Topaz area is nearly similar in thickness. It can therefore be categorized as carbonate platform. Carbonate platform is a general term. It is used to refer to carbonate sequences developed in a range of geotectonic settings and also to any depositional surface upon which shallow-water carbonate facies are deposited (Pomar, 2001).

Well Seismic Tie

Well-seismic tie is generated to identify top and bottom horizon of Baturaja Formation in the seismic (Figure 4). The real depth position of seismic section was estimated and correlated to well data by well seismic tie. The density and sonic logs (calibrated with checkshot surveys) were used based on three wells. The derived reflectivities were then convolve with the minimum phase wavelet extracted from the seismic data to generate synthetic seismograms that was then correlated to the corresponding seismic traces. The synthetic seismograms were able to obtain a good character match for the top and bottom horizon of Baturaja Limestone.

Horizon and Structural Interpretation

The cycles of Baturaja Limestone can be identified and correlated from the wells. Unfortunately, these cycles do not correspond to discrete events in the seismic data and so were not mappable seismically. Top of Baturaja Limestone is characterized by zero crossing from positive to negative amplitude, corresponding to the shale-carbonate contact at the top of the formation. Bottom of Baturaja Limestone is characterized by zero crossing from negative to positive amplitude due to carbonate-sandstone contact at the bottom of the formation (SEG normal polarity). Red and blue colors correspond to changes in peak and trough amplitudes respectively, and the Baturaja Limestone at study area lies on trough amplitude. Faulted and folded Baturaja Limestone developed at Topaz area (Figure 5). Kyanite area located above the basement high (horst) was isolated by normal fault in the surrounding area. Meanwhile, Pyroxene area was located above the basement low (graben) where the thick syn-rift sediment accumulated below the Baturaja Limestone. Similar characteristic with well correlation, the seismic interpretation of Baturaja Limestone at 3D Topaz area shows that, in the entire area, the carbonates are almost similar in thicknesses. Cutting and core description from Topaz-5 well indicating the development of reefal facies (as indicated by the existence of boundstone). However, this characteristic was not clearly observed from the seismic section. Instead, this reefal facies was identified as low relief reef within carbonate platform.

Time Attibutes for Structural Interpretation

Time-derived attributes help to discern structural detail. Based on the interpreted three dimensional surface defined by the horizon, a number of attributes which highlight the effects of faults or other discontinuities can be mapped on the horizon. The interpretation of fault traces on the horizon then becomes a process of lineament interpretation on images of various types of data mapped along the horizon of interest. Variance cube volume attribute improves the accuracy of the structural and stratigraphic interpretation rather than the inferred similarity of seismic data (Figure 6).

Depth Structure and Isopach Map

Depth structure map at top Baturaja Limestone at 3D topaz area exhibits several anticlines bounded by Pre-Tertiary and Tertiary fault system (Figure 7). The faults are bordered at northern and southern part of the area and have direction similar to Barisan or Semangko trend. The Pyrite area also displays similar configuration with Tourmaline area. The Topaz area exhibits the anticline which is bounded by the NS trending fault system, especially for

Topaz-3, Topaz-4, and Topaz-5 wells. Kyanite area can be divided into northern and southern parts separated by few faults which follow the Barisan or Semangko trend. Major faults at reservoir scale are better imaged on seismic section then displayed at depth on the structure map. It shows the orientation of minor faults and fractures zone that may affect the reservoir quality. The developmet of faults at 3D Topaz area can play an important role as structural trap for hydrocarbon accumulation and capable to enhance the reservoir quality of Baturaja Limestone. Isopach maps have many uses in regional geology. They are used to locate buried structures and to indicate the direction of probable wedging, as well as help to restore the original depositional edge of the stratigraphic unit.

Amplitude Envelope

The porous zone interval was estimated from well log analysis. Conversion from depth to time was done by synthetic seismogram at Pyrite-5 (Figure 8). The average porous zone interval in wells at the study area is about 50 meter below top of Baturaja Limestone which is equivalent to 20 milisecond in time. This calculation will be used in slicing porous zone interval at 3D Topaz area.

Amplitude Envelope is used as a basic indicator of lithology/porefil. Sharp changes in amplitude envelope are often associated with sharp change in lithology. This attribute does not have enough vertical resolution but gives better lateral resolution. Figure 9 below shows the amplitude envelope map from top Baturaja Formation to 20 ms below. Amplitude variation shown in this figure depicts different facies distribution. Low amplitude value is usually related to the porous area and high amplitude value related to the tight area in Baturaja Limestone. The amplitude envelope shows more porous area at eastern part and tight area at western part. The porous area corresponds to wackstone/packstone in carbonate platform while the tight area corresponds to mudstone/wackstone in carbonate platform. Based on cutting and core dercription, there observed a reefal facies in the middle part of 3D Topaz area. However, this cannot be seen from the amplitude envelope result. This is due to the fact that the reefal part has the same amplitude level with wackstone/packstone. The porosity in the carbonate platform already is enhanced due to subaerial exposure in the entire area. However, the porosity enhancement caused by the faulting only occured at certain location. The fracture enhanced porosity has made the mudstone/wackstone area become a better place for hydrocarbon accumulation. This is demonstrated from low amplitude level observed at Tourmaline, Pyrite, and Pyroxene area. The fracturation process due to faulting development can also enhance the dissolution process. These areas have been proven to produce gas and condensate.

Frequency Decomposition

Various attributes described previously can only differentiate porous and non porous zones in carbonate platform at 3D Topaz area but not the facies distribution. Therefore, the frequency decomposition attribute was applied to the seismic data at study area. The top Baturaja horizon was chosen as the target and different frequency was analyzed to get the best frequencies which can reveal a meaningful image of subsurface.

Three frequencies were used to blend by using the RGB blending tool, 20 Hz as low frequency is shown by red color, 30 Hz as middle frequency is shown by green color and 35 Hz as high frequency is shown by blue color. Figure 10 displays the result of frequency decomposition map using RGB blending tool. Based on RMS amplitude and amplitude envelope, the facies distribution of carbonate platform at 3D Topaz area are not clearly shown, but from the frequency decomposition integrated with cutting and core description, the carbonate platform can be differentiate into three main facies for paleoenvironment (Figure 11).

Fore reef, located at the eastern part (Biotite and Kyanite area) which contains wackstone/packstone. This facies is shown by red color from frequency decomposition map. South Kyanite area is located at the fore reef area, but it is displayed as white color which is quite different than surrounding. White color, in RGB blending, shows a combination between low, middle, and high frequencies. The white color at South Kyanite is interpreted as muddy facies development in the fore reef area. Some faults which separate between North Kyanite and South Kyanite has developed depression at South Kyanite, resulting in this area to be deeper than surrounding and consequently deposited more muddy limestone.

Low relief reef, located in the middle part (Topaz and Corondum area), contains boundstone/wackstone/packstone. This reef catch-ups from fore reef toward back reef. This facies is shown by dark red color. It can therefore be separated from the fore reef facies.

Back reef, located in the westen part (Tourmaline, Pyrite, Pyroxene, and Titanite area), contains mudstone/wackstone. This facies is shown by lighter red to blue color at some part.

Seismic Inversion

Seismic inversion was made as an attempt to quantitatively describe the reservoir properties such as porosity. The conversion from interface information (normal seismic amplitude) to interval information, by the virtue of seismic inversion, also brings the seismic data into a more geologic form readily correlated to well logs and to reservoir properties. In order to overcome the complexity of the area as shown by pervious seismic attributes, seismic inversion was run with initial model taken from three different key wells representing three different facies. The wells are Tourmaline-3, Pyrite-5, and Kyanite-16. These wells represent the mudstone/wackstone area for Tourmaline-3 and Pyrite-5, and wackstone/ packstone area for Kyanite-16. The relationship between impedance and porosity was recognized by cross-plotting the porosity and impedance in order to test the feasibility of applying seismic inversion. As is typical in carbonates, porosity and impedance exhibits an inverse linear correlation, i.e. increases in porosity are manifested as decreases in impedance. Figure 12 shows the negative relationship between average porosity and impedance were observed.

Sparse Spike Inversion

This study performs seismic inversion using the linear programming sparse spike inversion technique. However, in this case, the average bandlimited inversion result was used as the initial model. This approach was believed to produce a more representable initial model as compared to the conventional one. The linear programming sparse spike means the algorithm creates a sparse reflectivity that produces the best match between the derived synthetic and the seismic trace, subject to the constraint that the number of spikes should be a minimum (sparse). Figure 13 shows the sparse spike inversion result in vertical section view across Pyrite-5 well. Excellent match between well P-impedance and the resulted inversion is observed.

The sparse spike inversion map shows low acoustic impedance value at the center and eastern part while high acoustic impedance value at western part in the study area. The low acoustic impedance shows more porous carbonate platform than high acoustic impedance.

Porosity Map

Seismic inversion provides insight to porosity variations away from well control. This can be a valuable tool for reservoir characterization prior to field development. Prior to choosing the seismic inversion method which shows better correlation to average porosity (PHIA) from the well logs, cross ploting between acoustic impedance (AI) and PHIA in porous zone interval (from top BRF to 50 m below for porosity log and from top BRF to 20 ms below (for seismic inversion) has to be made. Porosity and impedance displays an inverse linear correlation, i.e. increases in porosity are manifested as decreases in impedance. Figure 14 below displays the correlation between impedance and PHIA at certain areas. The area located in the western part of the study area is dominated by mudstone/packstone. This area shows linear relationship pattern between impedance and porosity (porosity increase – impedance increase). The higher acoustic impedance (tight limestone) is related to the higher porosity which is mainly due to fracturation process (more brittle limestone). The linear relationship between impedance and porosity observed in this area will make a pitfall interpretation for producing porosity map. The center and western part of the study area is dominated by boundstone/wackstone/packstone and wackstone/packstone respectively. This area shows negative correlation pattern, means that the high acoustic impedance corresponds to the low porosity value, while the low acoustic impedance corresponds to the high porosity value. This trend then was used in cokriging geostatistic analysis to produce the porosity map at 3D Topaz area. The acoustic model from seismic inversion provides information from which predicted porosity values may be calculated, providing an accurate estimate of porosity away from the well locations. The cross plot between acoustic impedance from average bandlimited inversion and average porosity shows better cross-correlation than impedance from sparse spike inversion. Therefore, the average bandlimited inversion result was used to produce porosity map (Figure 14).

Figure 15 shows the porosity map produced from cokriging between average bandlimited inversion (as the secondary data) and average porosity from well log as the primary data. The porosity map shows porosity distribution at the 3D Topaz area. Some areas like Tormaline, Pyrite and Pyroxene, although dominated by mudstone/wackstone, still shows good porosity development. This is interpreted as due to fracturation created by fault development which enhances the secondary porosity of carbonate platform. Topaz area which is dominated by boundstone/ wackstone/packstone (low relief reef) show good porosity development. The reefal facies have originally good initial porosity, the dissolution process can however further enhanced the secondary porosity to make this area better in reservoir quality. The eastern part of the 3D Topaz area which is dominated by wackstone/packstone has good porosity development.

Integration Map

Integration map is required to determine the prospect and risk area for field development. Figure 16 displays the depth structure map at top BRF, isopach, frequency decomposition, and porosity map at study area. Based on the integration map, there observed three prospects and one risk area for field development at the 3D Topaz area. The first and second prospects area located at the back reef which is dominated by mudstone/wackstone. Depth structure map at top BRF shows the structural nosing feature with faults, and the isopach map displays thicker limestone at the first and second prospect area. Comparing with porosity map, both of the prospect areas have good porosity distribution due to dissolution and fracturation process. The third prospect area is located at low relief reef dominated by boundstone/wackstone/packstone. Depth structure map at top BRF shows structural anticline with fault. The porosity map shows good porosity distribution at this area due to initial porosity of low relief reefal facies and the secondary porosity like vuggy produced by dissolution process. Although South Kyanite area already has some wells, based on this study, this area is categorized as risk area for field development. We should be more carefully to develop South Kyanite area. Depth structure map at top BRF shows that the South Kyanite area is separated with North Kyanite area by faults. This fault has created the limestone at South Kyanite to be more muddy in the fore reef facies which is dominated by wackstone/packstone. Isopach map shows that this area has thinner limestone and exhibits low porosity distribution from porosity map. Integration map has been successfully utilized to identify best potential location for further development.

Conclusion

1. Based on log correlation, the Baturaja Formation at the 3D Topaz area can be generally divided into 2 cycles in deposition. The first cycle shows porous zone indicated by vuggy porosity in the upper part and non porous zone in the lower part, while the second cycle only shows non porous zone.

2. Variance cube attributes exhibit useful image for delineation of fault boundary.

3. Carbonate platform at the 3D Topaz area contains evidence of diagenesis due to subaerial exposure and fracturation process which enhance secondary porosity.

4. In this area, dissolution due to diagenesis does not contribute much in enhancing the porosity in mudstone/wackstone. However, the fracturation process due to faulting is interpreted to give better enhancement for mudstone/wackstone, such as observed in Tourmaline, Pyrite, and Pyroxene area

5. The facies distribution of carbonate platform at 3D Topaz area are not clearly seen from RMS amplitude and amplitude envelope, but from the frequency decomposition which is integrated with cutting and core description, the carbonate platform can be differentiated into 3 facies:
   - Fore reef, located at the eastern part, which contains wackstone/packstone.
   - Low relief reef, located at the middle part, which contains boundstone/wackstone/packstone. This reef catch ups from fore reef toward back reef.
   - Back reef, located at the western part, which contains mudstone/wackstone.

6. The fore reef and low relief reef facies generally shows low acoustic impedances, while the back reef shows high acoustic impedances with the exception observed in the areas which are affected by faults. The latter exhibits good porosity due to the fracturation process.

7. Integrated analyses involving various seismic attributes including frequency decomposition and seismic inversion combined with well core and cutting description has been utilized to determine the prospect and risk areas for further field development.

Selected References

Abriel, W.L., 2008, Reservoir Geophysics: Applications: SEG, Tulsa, Oklahoma, 136 p.

Barnes, A., 2006, Too Many Seismic Attributes: CSEG Recorder, p. 40-45.

Bishop, M.G., 2001, Petroleum System of Northwest Java Province, Java and Offshore Southeast Sumatra, Indonesia: Colorado, U. S. Geological Survey. Open-File Report 90-50-S. Web accessed 3 January 2012, http://pubs.usgs.gov/of/1999/ofr-99-0050/OF99-50S/OF99-50S.pdf

Chambers, R.L., J.M. Yarus, and K.B. Hird, 2000, Petroleum Geostatistics for Non-Geostatistics, The Leading Edge, v. 19/5, p. 474-479.

Chopra, S., and K.J. Marfurt, 2008, Introduction to This Special Section - Seismic Attributes: The Leading Edge, v. 27/3, p. 296-297.

De Coster, G.L., 1974, The Geology of the Central and South Sumatra Basins: Oil and Gas Sydney, v. 20/9, 19 p.

Dunham, R.J., 1962, Classification of carbonate rocks according to depositional texture, *in*, Ham, W.E. (ed.), Classification of carbonate rocks: AAPG Memoir, v. 1, p. 108-121.

Jarvis, K., 2006, Integrating Well and Seismic Data for Reservoir Characterization: Risks and Rewards: Australian Earth Sciences Convention (AESC), Melbourne, Australia, 4 p. Web accessed 3 January 2012, http://www.fugro-jason.com/readingroom/techpapers/Integrating_Well_and_Seismic_2006_AESC_Jarvis.pdf

Liner, C.L., 2004, Elements of 3D Seismology, 2nd Edition: PennWell Publishing Company, Tulsa, U.S.A., 608 p.

Lines, L.R. and S. Treitel, 1984, A review of least-squares inversion and its application to geophysical problems: Geophysical Prospecting, v. 32/2, p. 159-186.

Pertamina BPPKA, 1997, Petroleum Geology of Indonesia Basin, Principle, Methods and Application: Volume X, South Sumatra Basin, Pertamina BPPKA.

Pertamina EP, 2006, Presentation Report of South Sumatra Basin: Unpublished.

Pomar, L., 2001, Types of Carbonate Platforms; A Genetic Approach: Basin Research, v. 13/3, p. 313–334.

Pulunggono, A and N.R. Cameron, 1984, Sumatra Microplates, their Characteristic and their Roll in the Evolution of the Central and South Sumatra Basins: 13th Annual IPA Proceedings, v. 1, p. 121-143.

Reading, H.G., 1996, Sedimentary Environment: Processes, Facies and Stratigraphy: Blackwell, Oxford, 688 p.

Robertson, J.D., and D.A. Fisher, 1988, Complex Seismic Trace Attributes: The Leading Edge, v. 7, p. 22-26.

Selley, R.C., 1998, Elements of Petroleum Geology, Second Edition: Academic Press, San Diego, CA., 470 p.

Sukmono, S., 2007, Seismic Course: Amplitude and Times Attributes for Reservoir Analysis: Dept. of Geophysical Engineering – ITB, Unpublished.

Sukmono, S., 2007, Application of multi-attribute analysis in mapping lithology and porosity in the Pmatang-Sihapas Groups of central Sumatra Basin, Indonesia: Leading Edge, v, 26/2, p. 126-131.

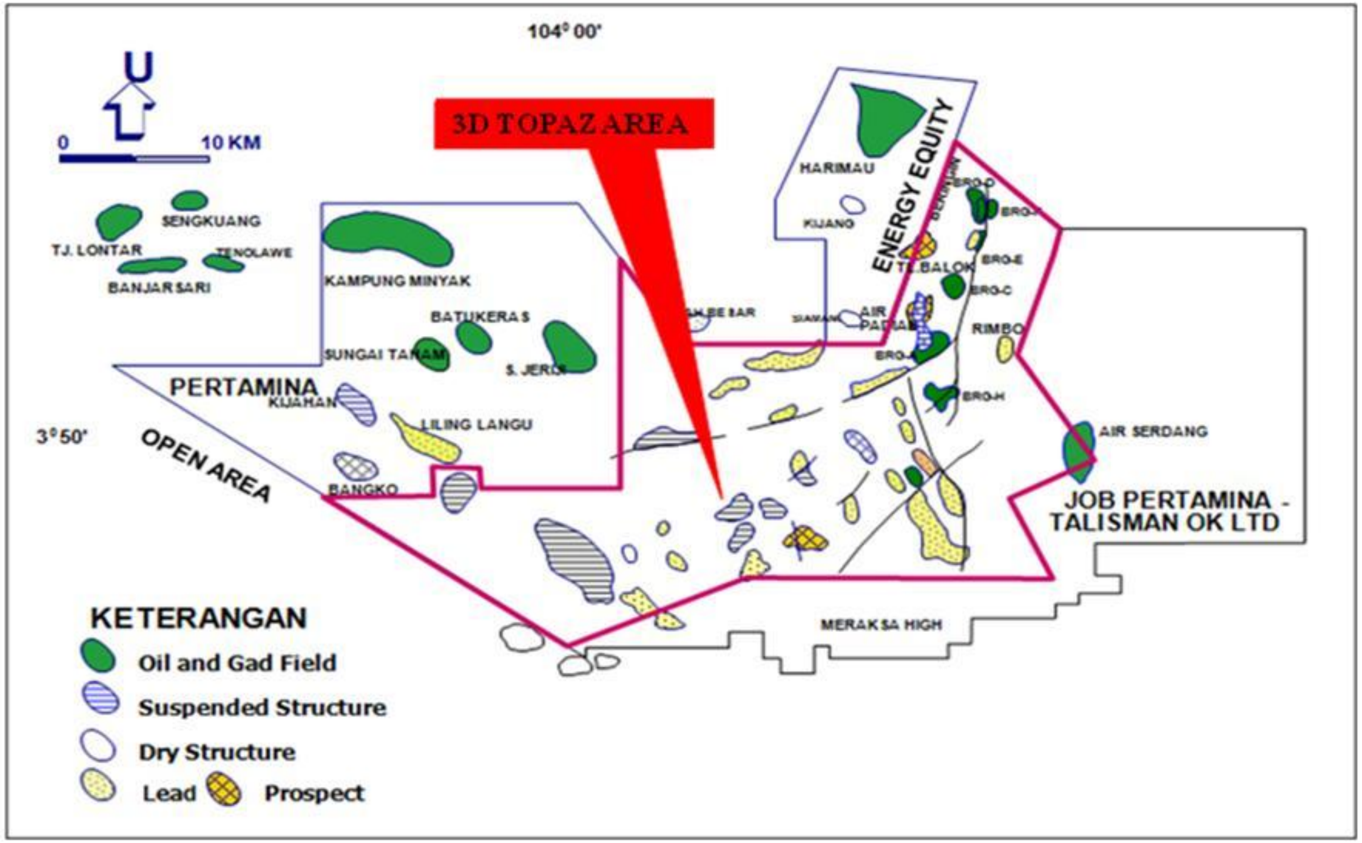

Figure 1. Location of study area (Pertamina EP, 2006).

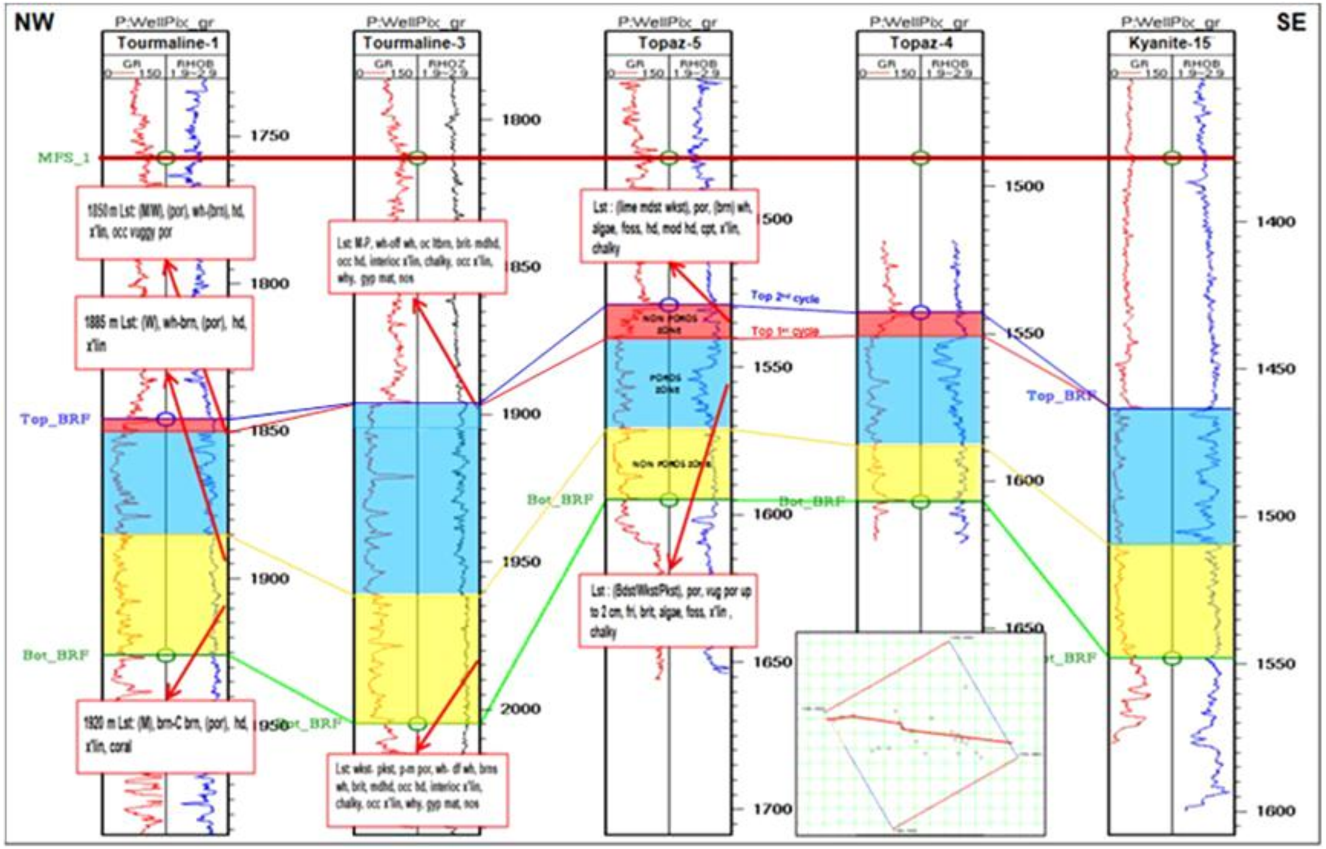

Figure 2. NW-SE well stratigraphy correlation of Baturaja Formation.

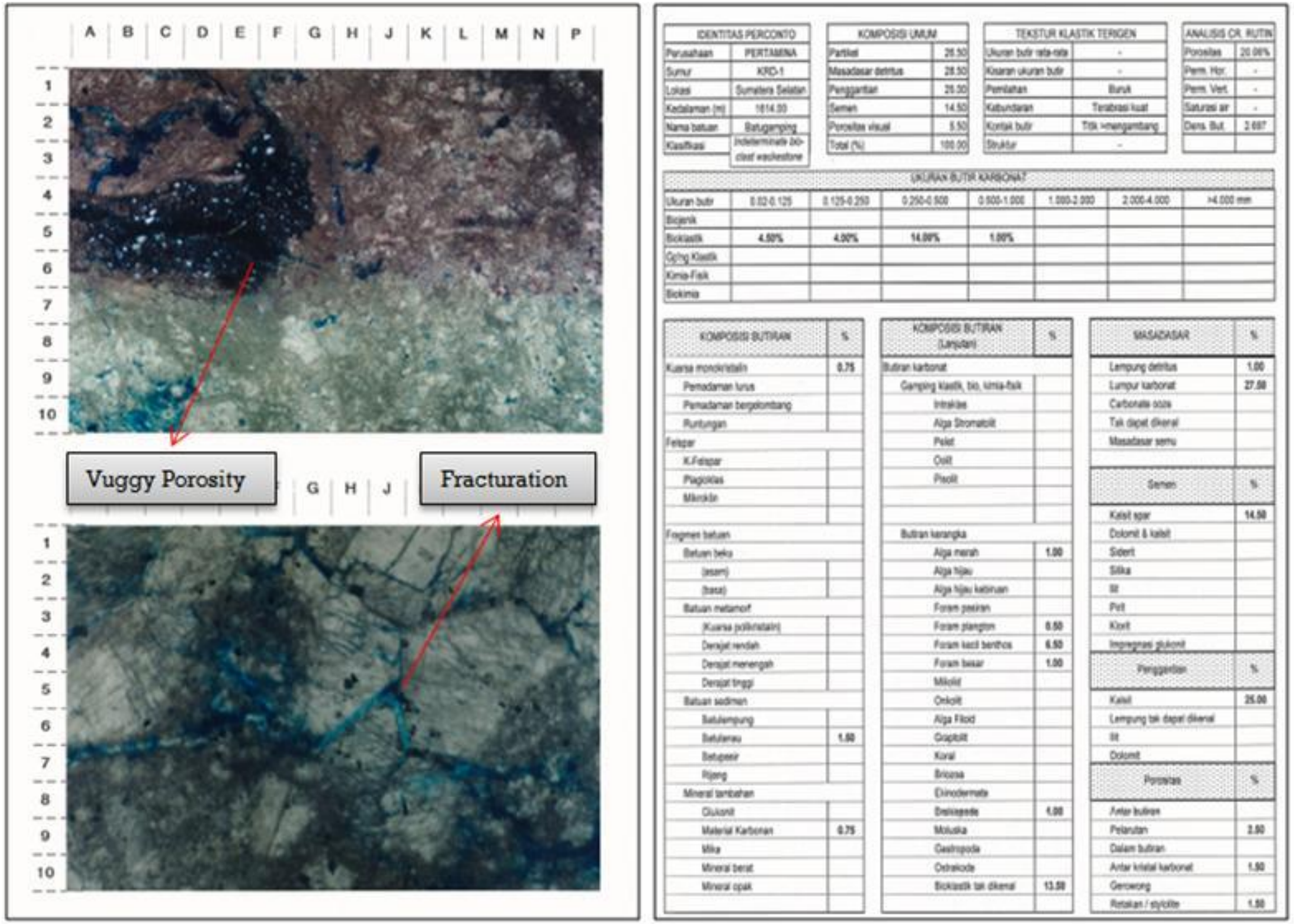

IDENTITAS PERCONTO	
Perusahaan	PERTAMINA
Sumur	KRD-1
Lokasi	Sumatera Selatan
Kedalaman (m)	1614.00
Nama batuan	Batugamping
Klasifikasi	Indeterminate bio-clast wackestone

KOMPOSISI UMUM	
Partikel	26.50
Masadasar detritus	28.50
Penggantian	25.00
Semen	14.50
Porositas visual	5.50
Total (%)	100.00

TEKSTUR KLASTIK TERIGEN	
Ukuran butir rata-rata	-
Kisaran ukuran butir	-
Pemilahan	Buruk
Kebundaran	Terabrasi kuat
Kontak butir	Titik +mengambang
Struktur	-

ANALISIS CR. RUTIN	
Porositas	20.06%
Perm. Hor.	-
Perm. Vert.	-
Saturasi air	-
Dens. But.	2.687

UKURAN BUTIR KARBONAT							
Ukuran butir	0.02-0.125	0.125-0.250	0.250-0.500	0.500-1.000	1.000-2.000	2.000-4.000	>4.000 mm
Biojenik							
Bioklastik	4.50%	4.00%	14.00%	1.00%			
Gp'ng Klastik							
Kimia-Fisik							
Biokimia							

KOMPOSISI BUTIRAN	%
Kuarsa monokristalin	0.75
Pemadaman lurus	
Pemadaman bergelombang	
Runtungan	
Felspar	
K-Felspar	
Plagioklas	
Mikroklin	
Fragmen batuan	
Batuan beku	
(asam)	
(basa)	
Batuan metamorf	
(Kuarsa polikristalin)	
Derajat rendah	
Derajat menengah	
Derajat tinggi	
Batuan sedimen	
Batulempung	
Batulanau	1.50
Batupasir	
Rijang	
Mineral tambahan	
Glukonit	
Material Karbonan	0.75
Mika	
Mineral berat	
Mineral opak	

KOMPOSISI BUTIRAN (Lanjutan)	%
Butiran karbonat	
Gamping klastik, bio, kimia-fisik	
Intraklas	
Alga Stromatolit	
Pelet	
Ooit	
Pisolit	
Butiran kerangka	
Alga merah	1.00
Alga hijau	
Alga hijau kebiruan	
Foram pasiran	
Foram plangton	0.50
Foram kecil benthos	6.50
Foram besar	1.00
Mikolit	
Onkolit	
Alga Filoid	
Graptolit	
Koral	
Briozoa	
Ekinodermata	
Brakiopoda	1.00
Moluska	
Gastropoda	
Ostrakoda	
Bioklastik tak dikenal	13.50

MASADASAR	%
Lempung detritus	1.00
Lumpur karbonat	27.50
Carbonate ooze	
Tak dapat dikenal	
Masadasar semu	
Semen	**%**
Kalsit spar	14.50
Dolomit & kalsit	
Siderit	
Silika	
Ilit	
Pirit	
Klorit	
Impregnasi glukonit	
Penggantian	**%**
Kalsit	25.00
Lempung tak dapat dikenal	
Ilit	
Dolomit	
Porositas	**%**
Antar butiran	
Pelarutan	2.50
Dalam butiran	
Antar kristal karbonat	1.50
Gerowong	
Retakan / stylolite	1.50

Figure 3. Petrography analysis Corondum-1 well at 1614 m.

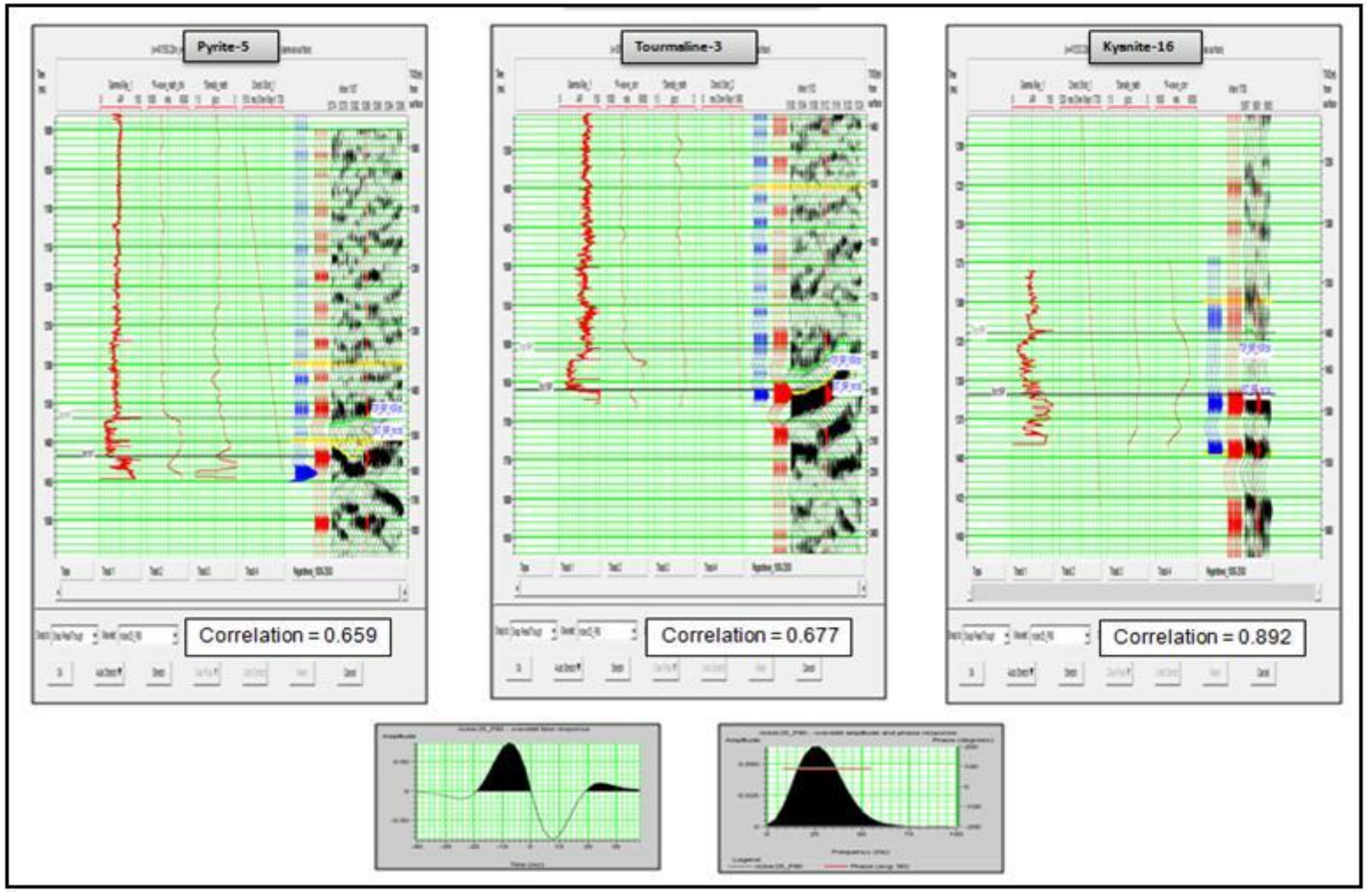

Figure 4. Well seismic ties for three wells and their correlation.

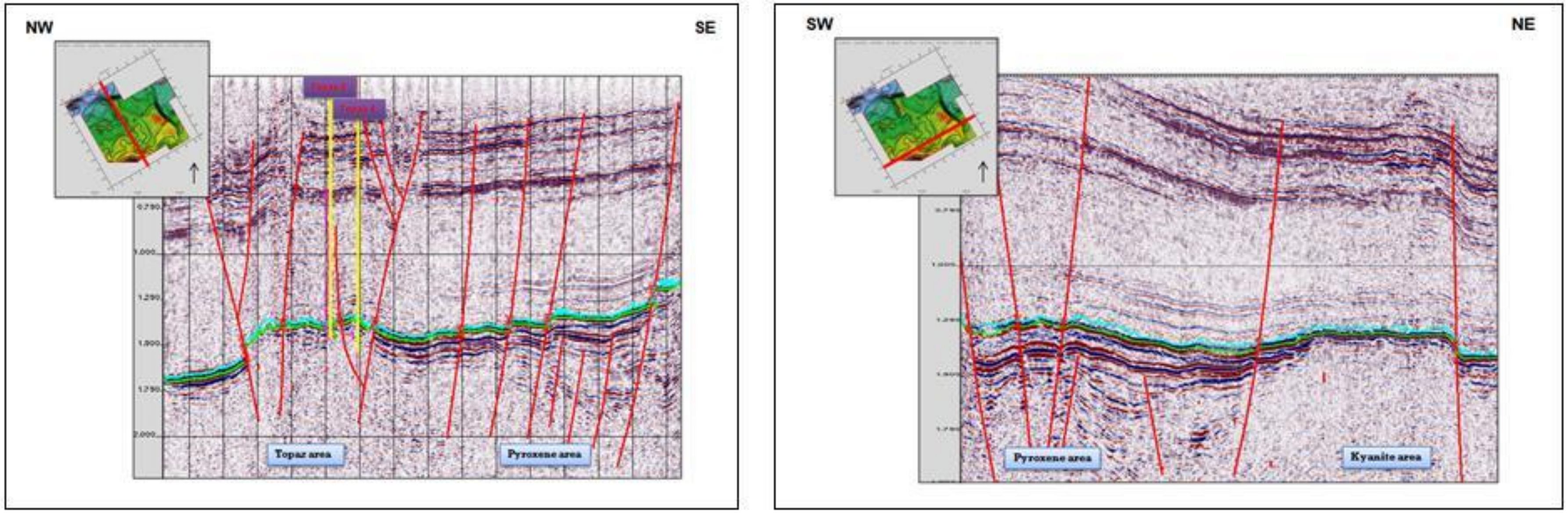

Figure 5. Seismic interpretation at line NW-SE and line SW-NE.

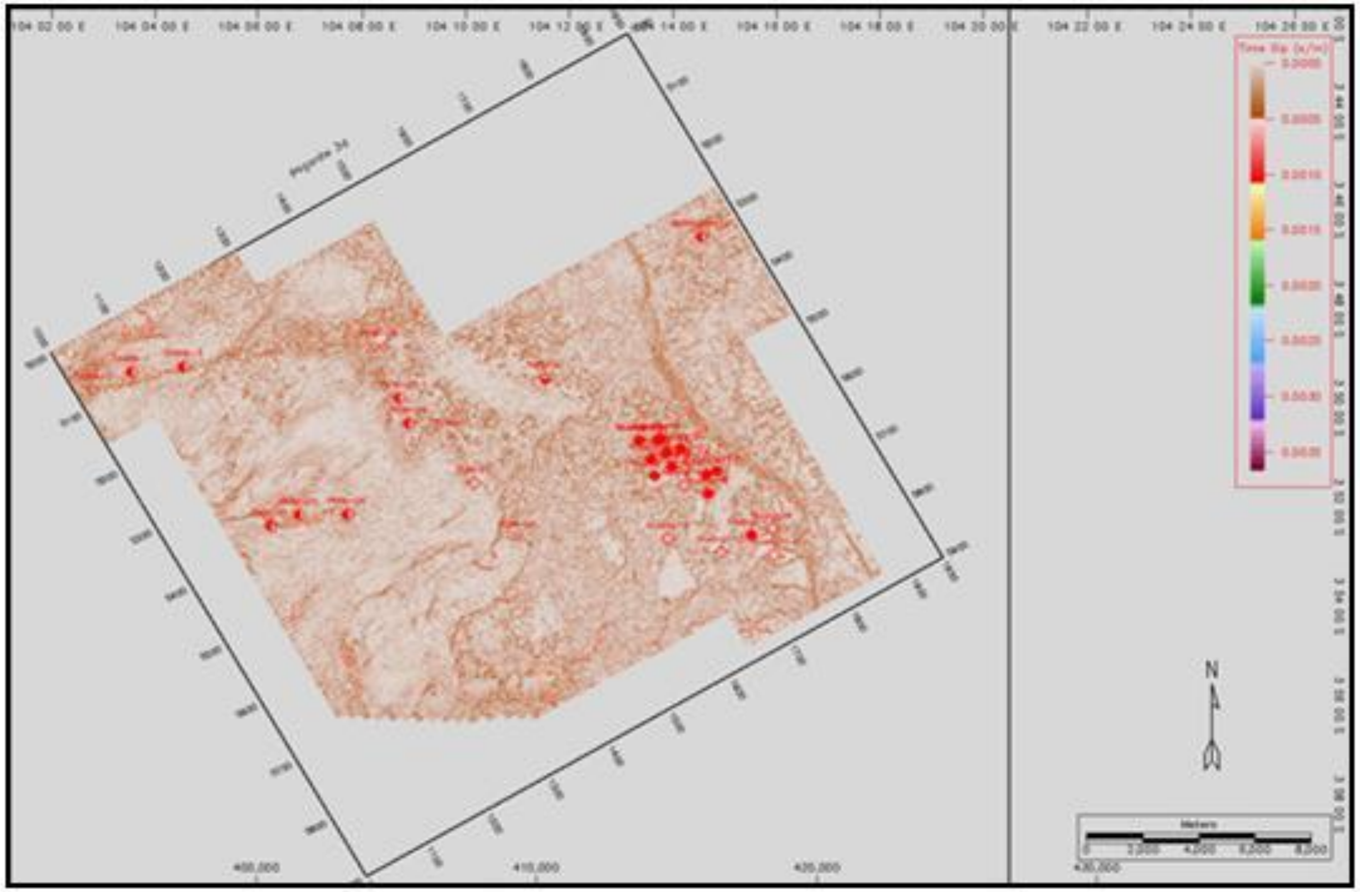

Figure 6. Variance attribute map at top Baturaja Formation.

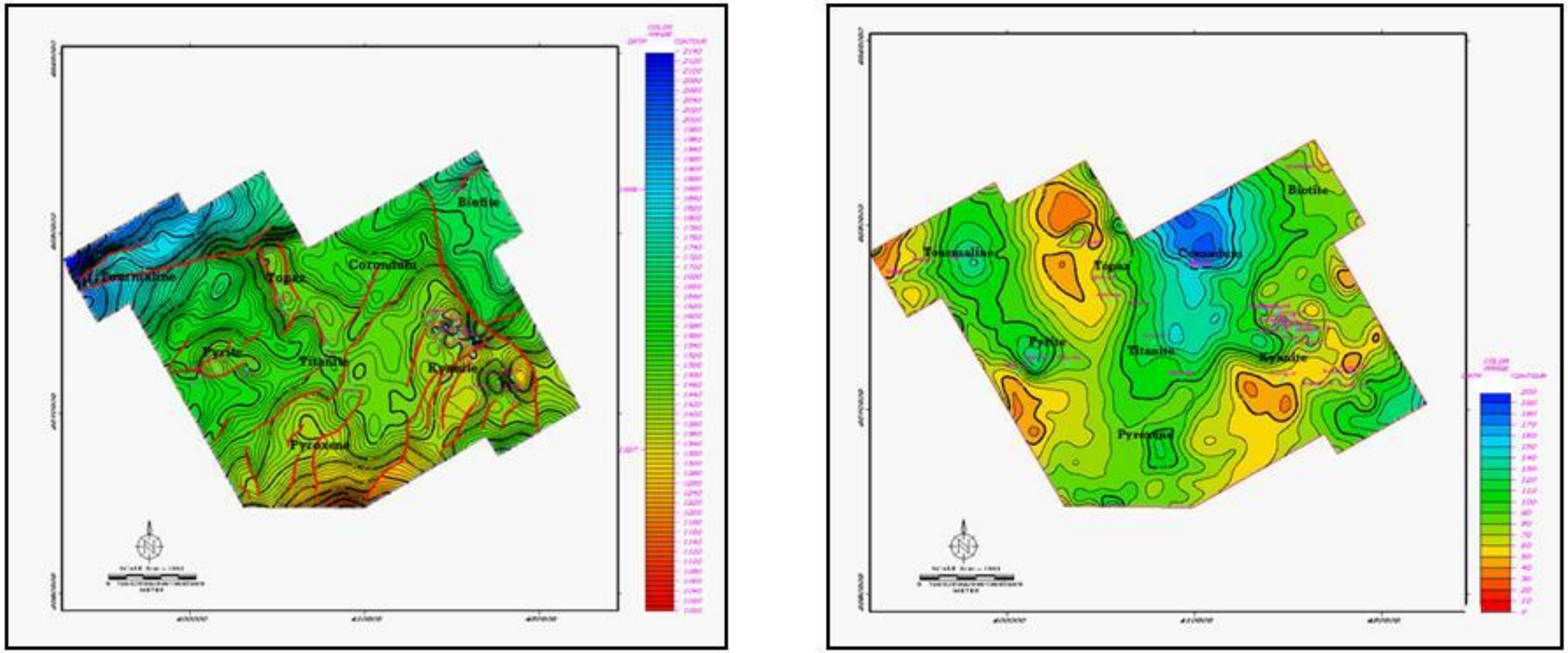

Figure 7. Depth structure map at top Baturaja & isopach map Baturaja.

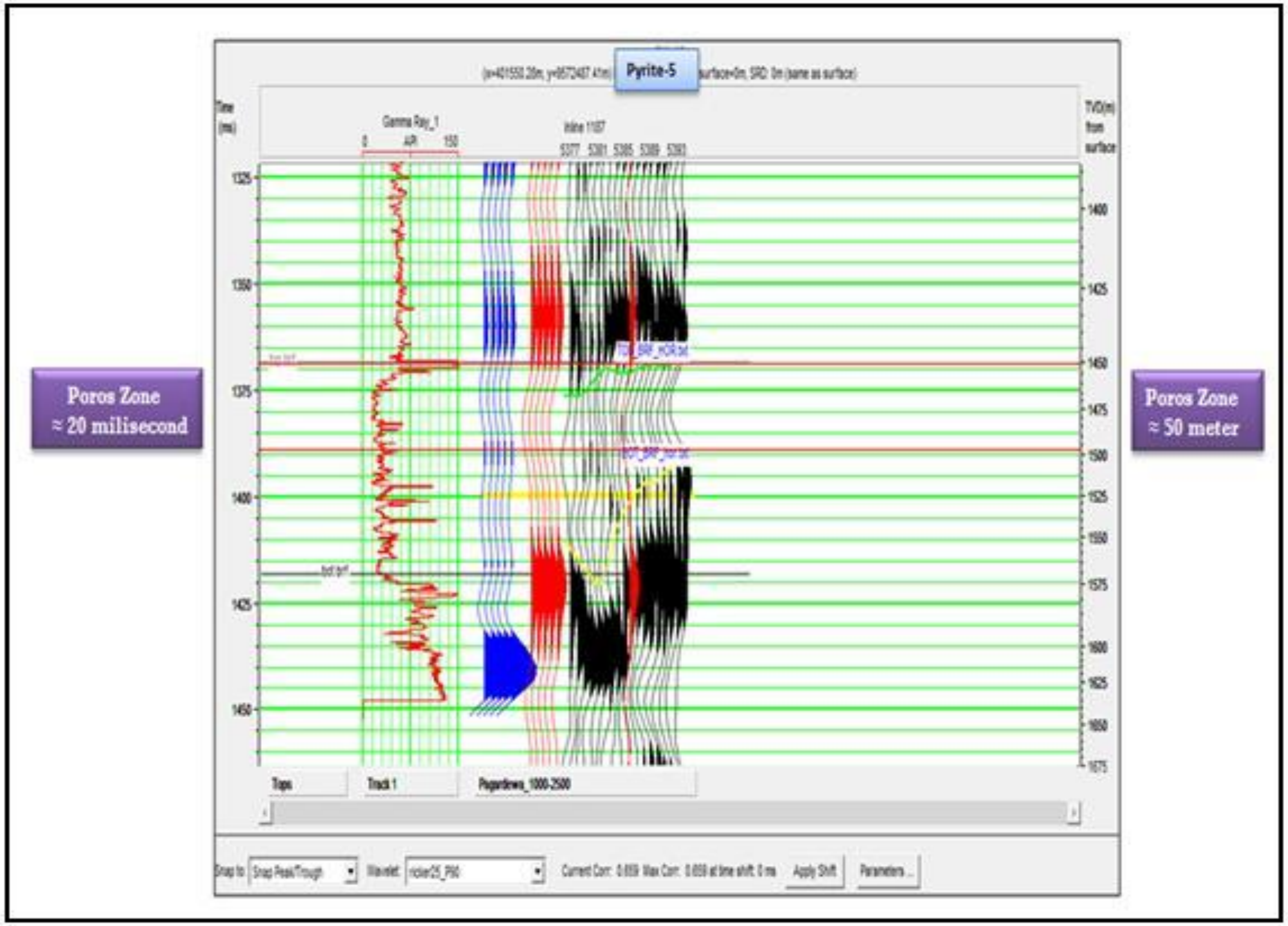

Figure 8. Converting depth to time for poros zone.

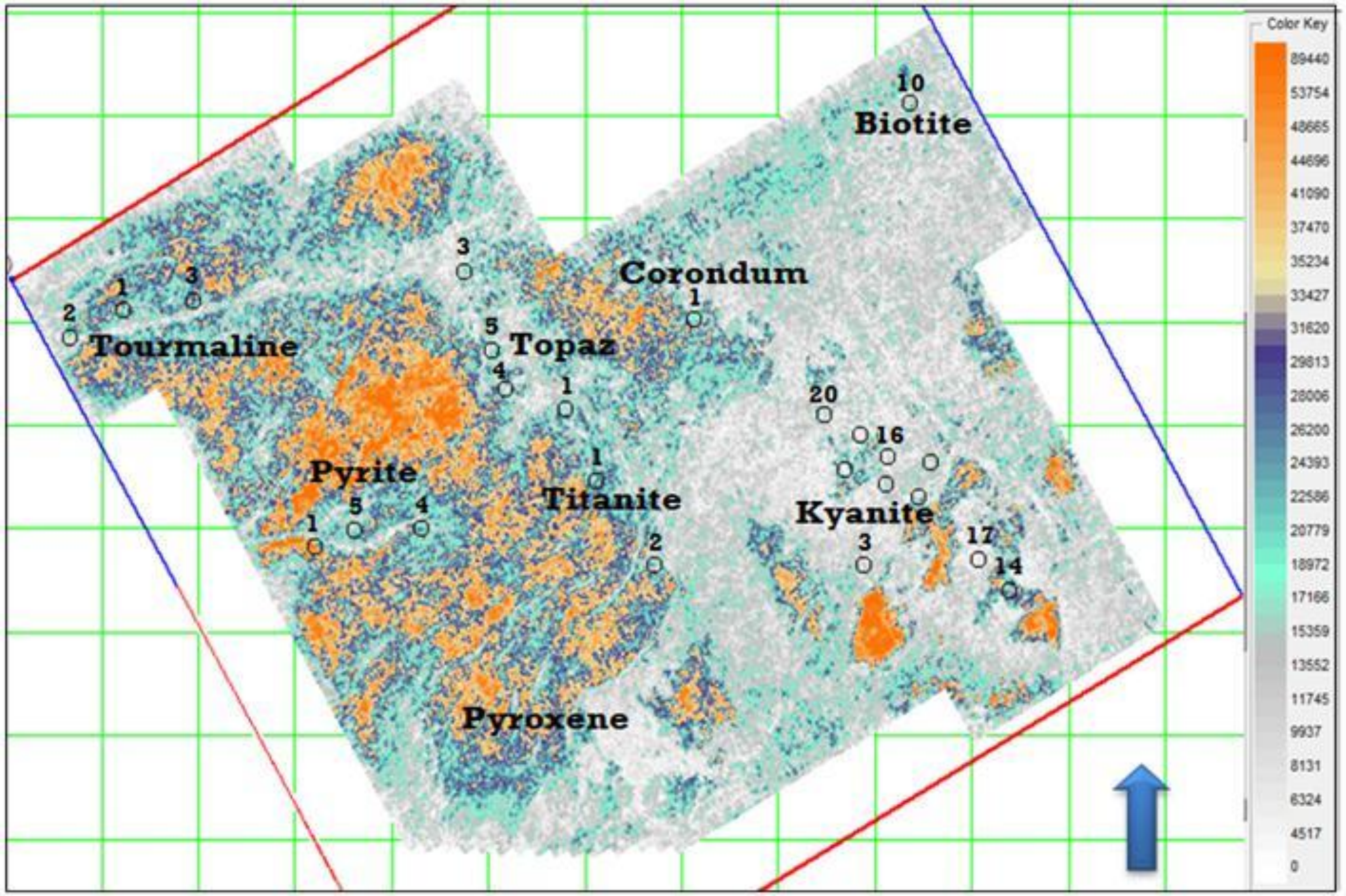

Figure 9. Amplitude envelope map from Top BRF to 8 ms below.

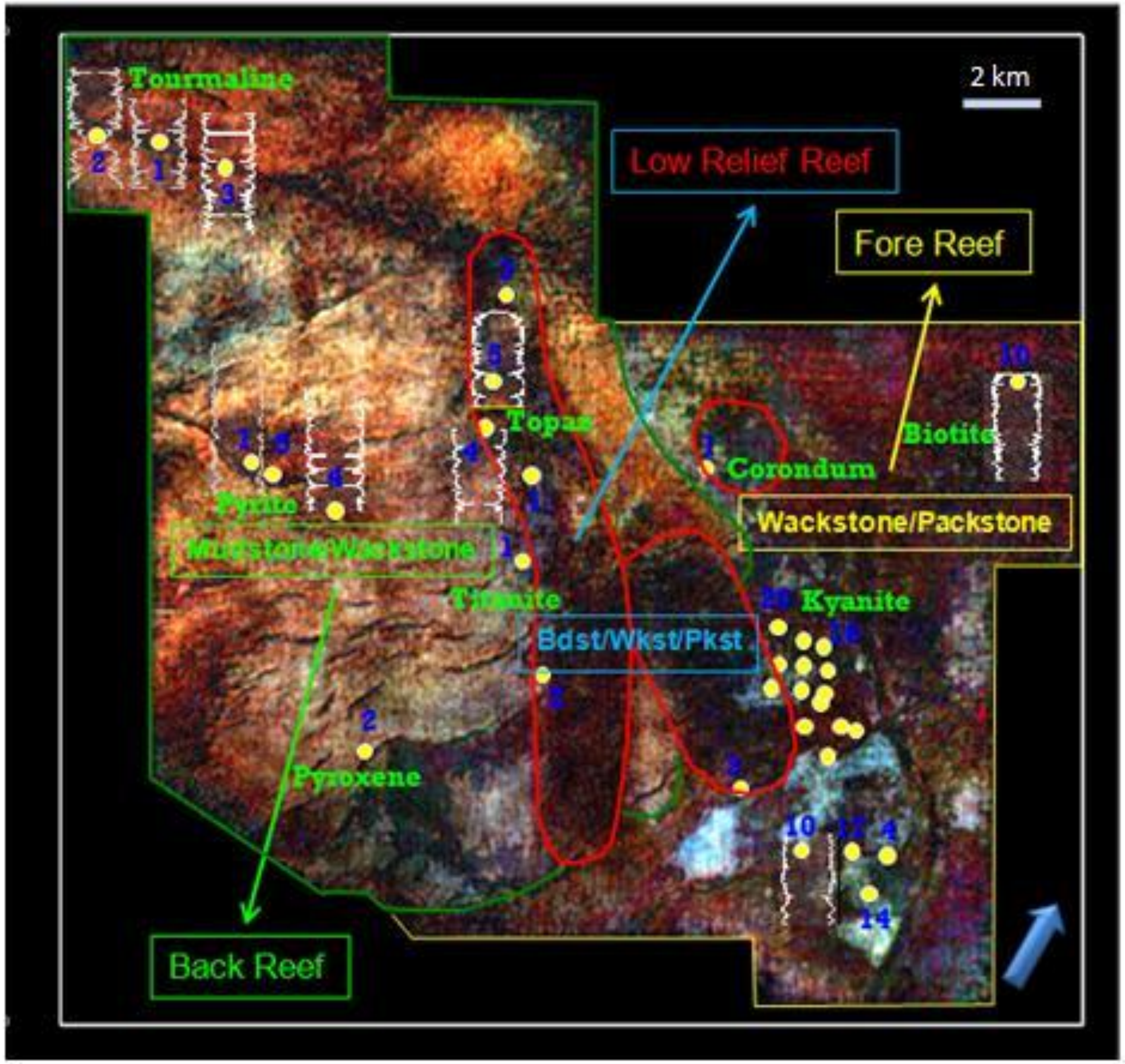

Figure 10. Frequency decomposition using RGB blending

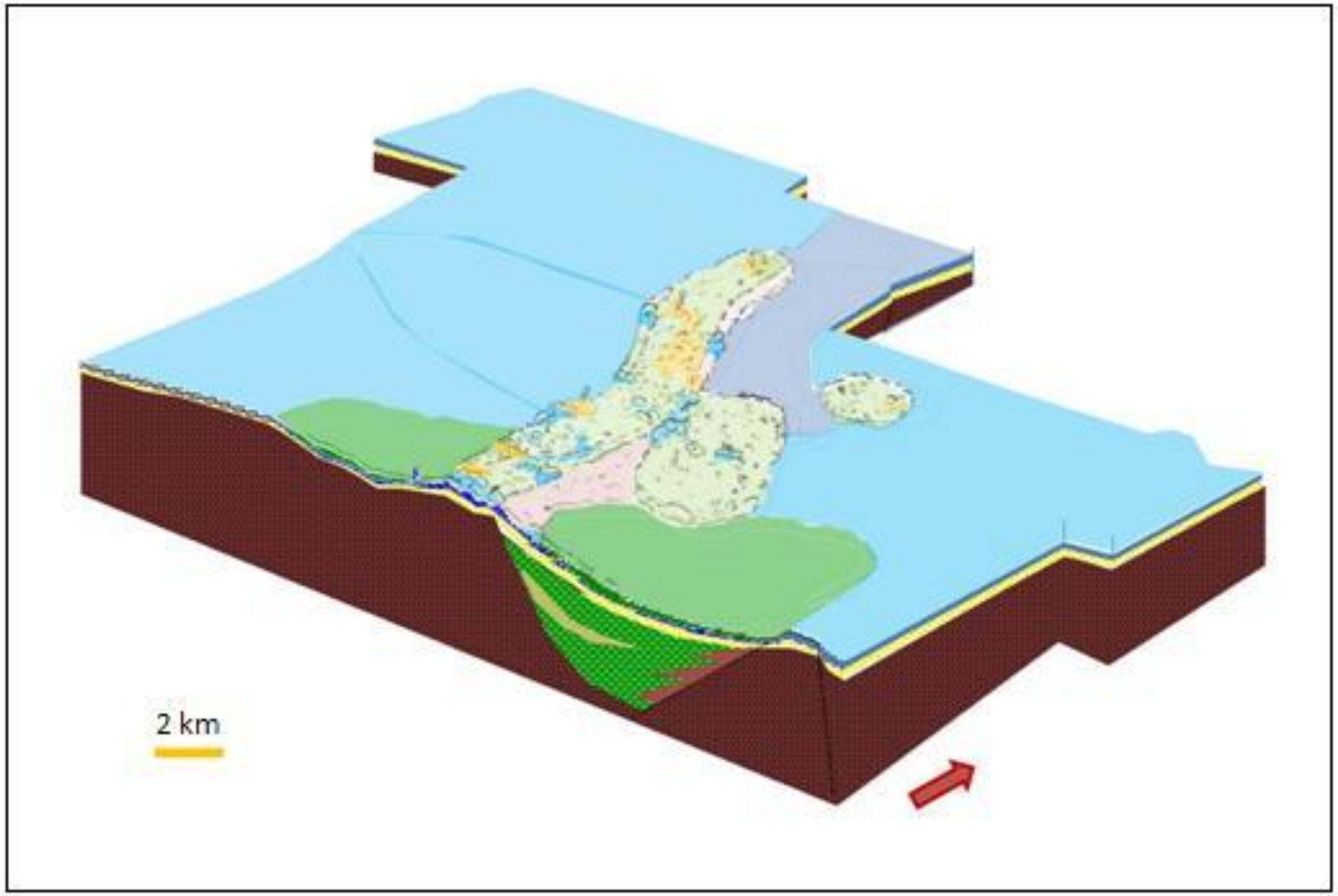

Figure 11. Paleoenvironment of Pagar Dewa Area.

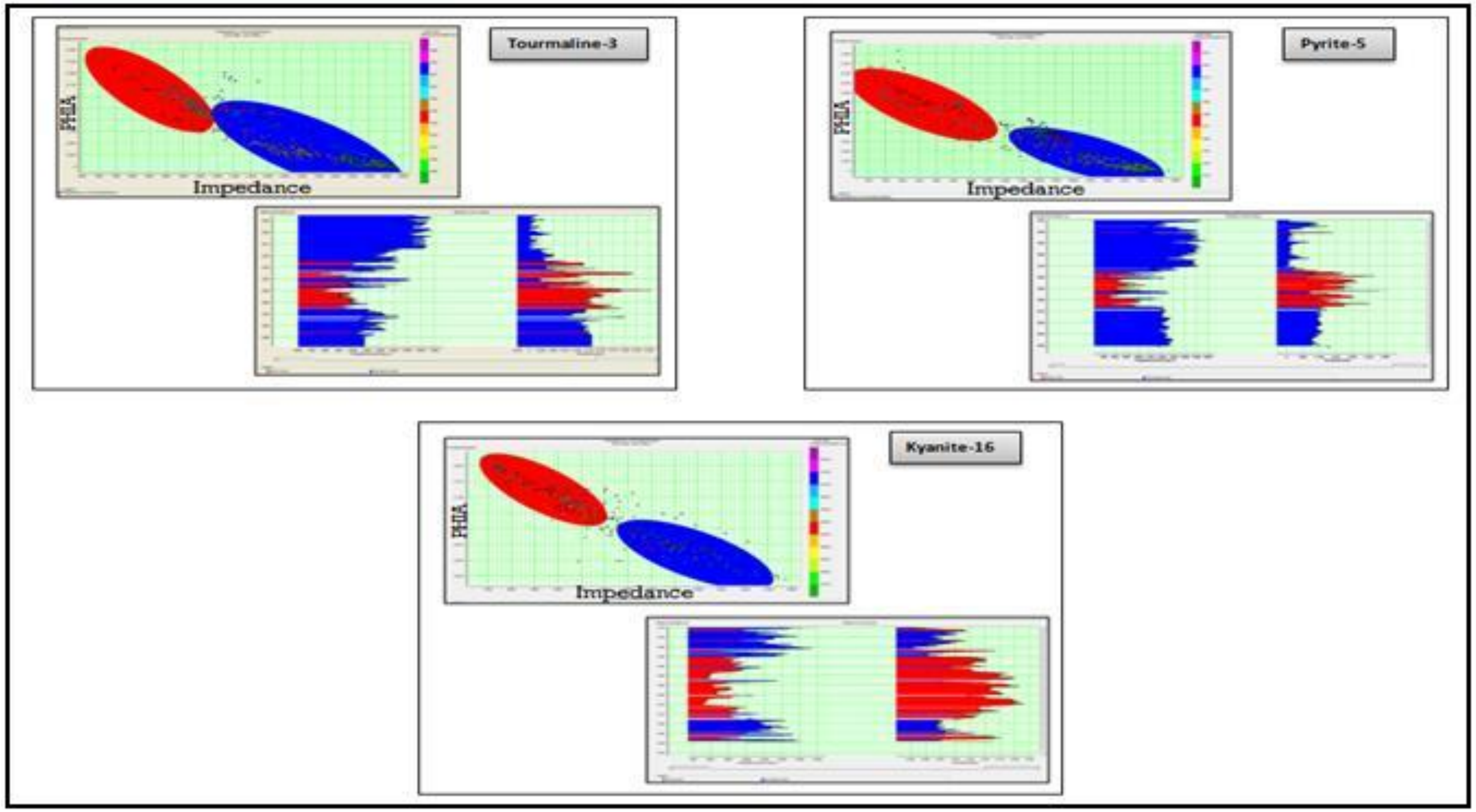

Figure 12. Cross plot between average porosity and impedance for three wells.

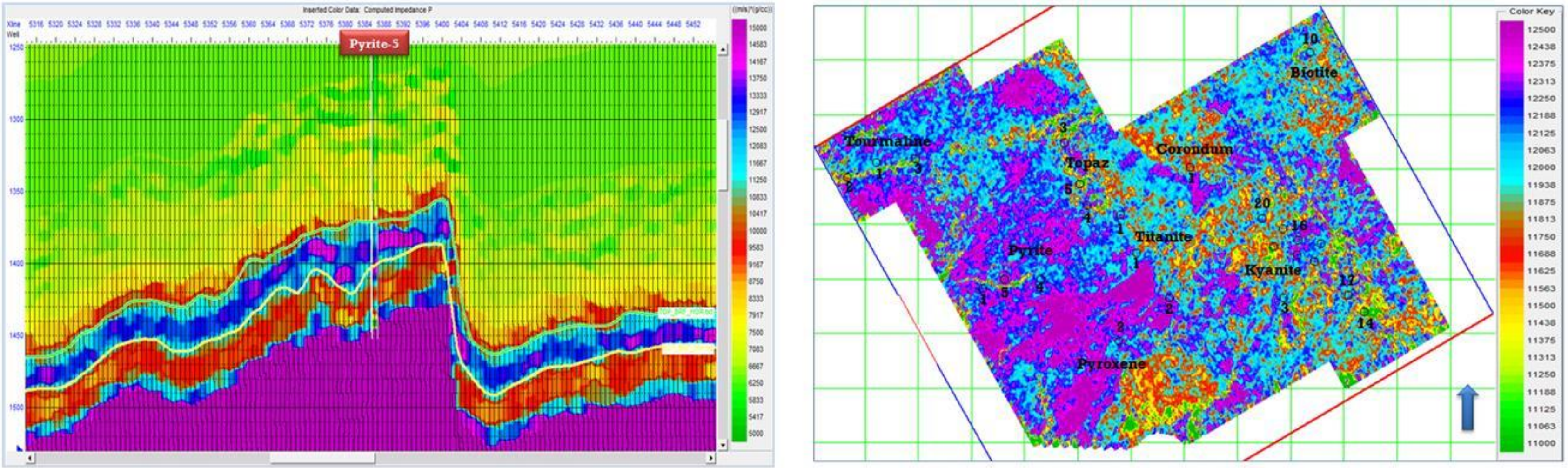

Figure 13. Sparse spike inversion section & map from top BRF to 20 ms below.

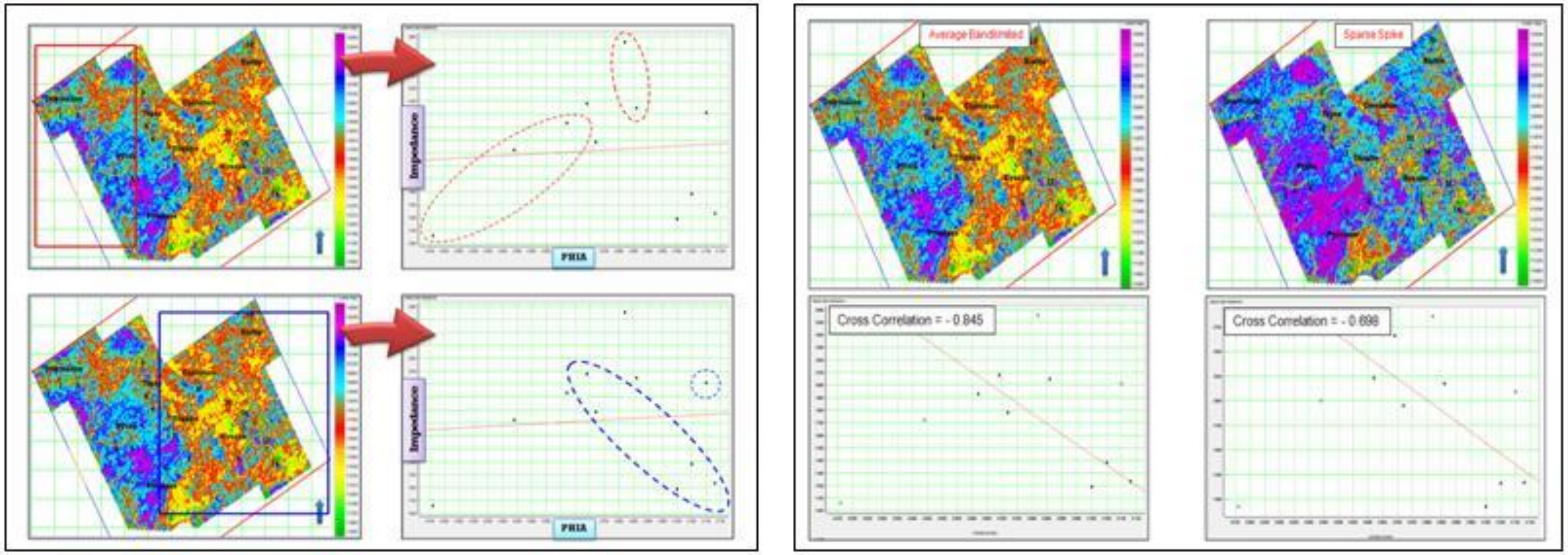

Figure 14. Cross plot between acoustic impedance and PHIA & comparison between bandlimited and sparse spike inversion.

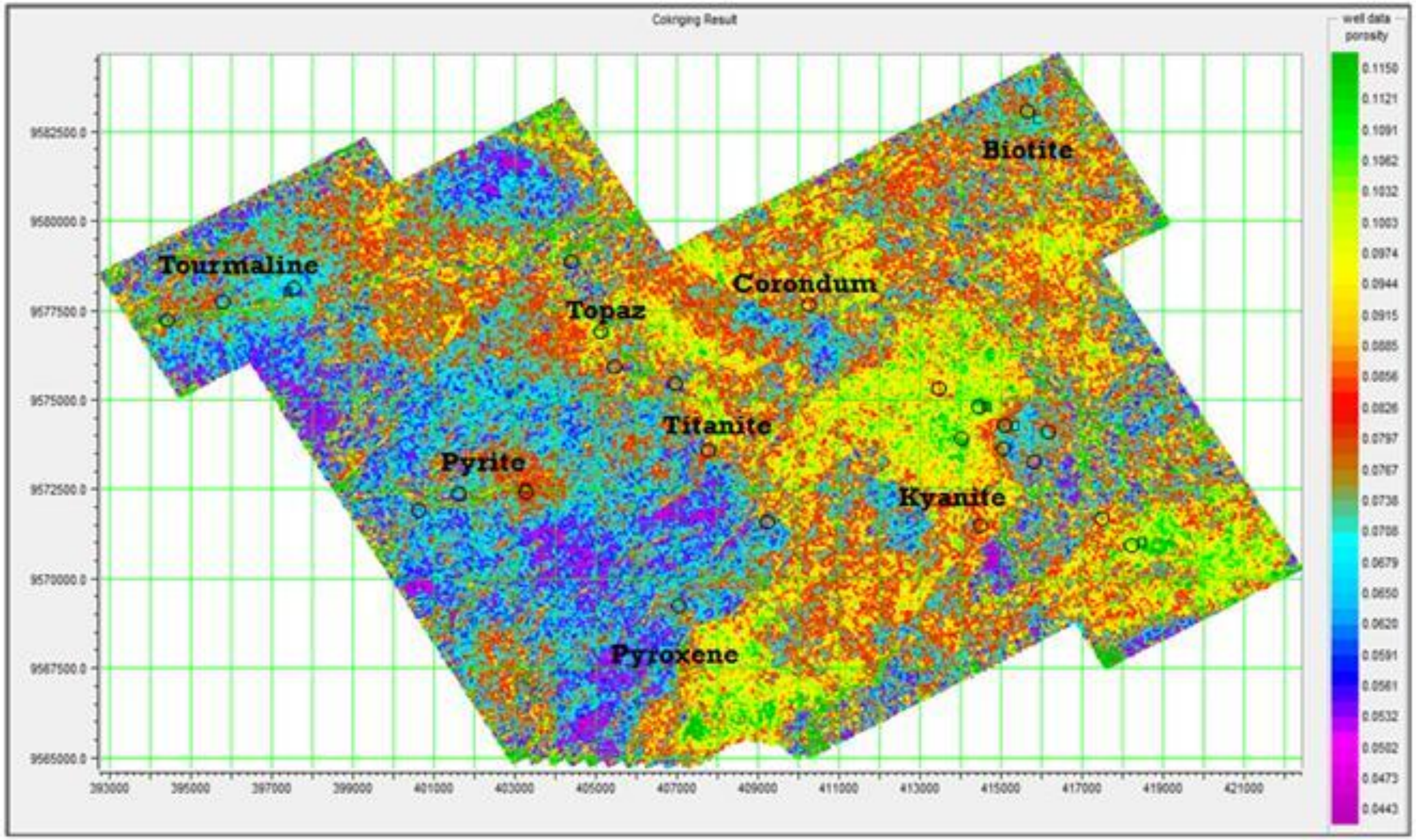

Figure 15. Porosity map from cokriging result.

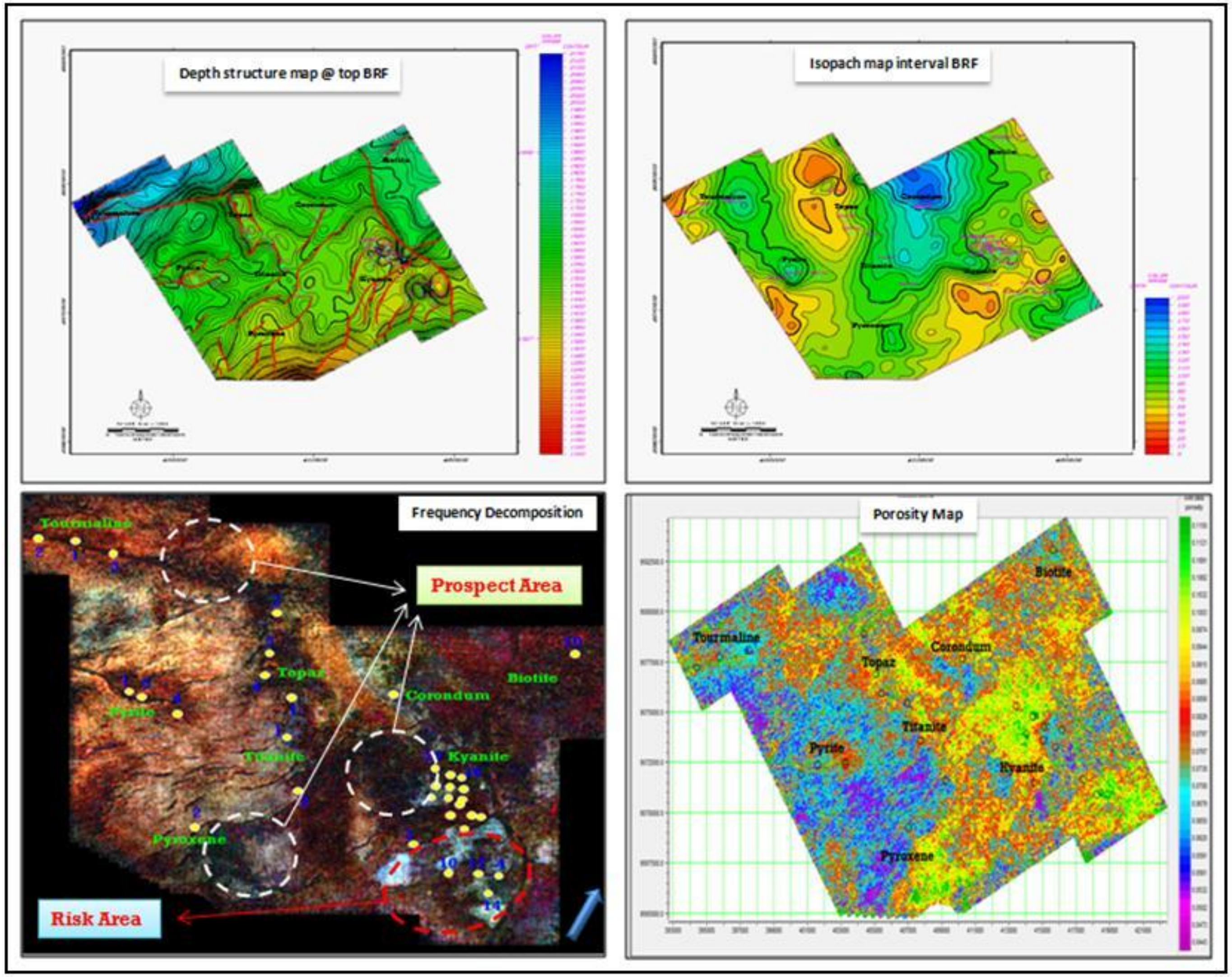

Figure 16. Integration map for field development.